

# Isotopic Tracing of Phosphorus Fraction Distribution in Chinese Fir Seedlings with High Phosphorus Efficiency Using $^{32}\text{P}$ Labelling

Xianhua Zou

Qingqing Liu

Zhijun Huang

Sitong Chen

Pengfei Wu

Xiangqing Ma (✉ [lxymxq@126.com](mailto:lxymxq@126.com))

Fujian Agriculture and Forestry University <https://orcid.org/0000-0003-3097-2372>

---

## Research Article

**Keywords:** Chinese fir, total P, P fractions, high- and low- P treatments, isotopic tracking

**Posted Date:** April 20th, 2022

**DOI:** <https://doi.org/10.21203/rs.3.rs-1560791/v1>

**License:**   This work is licensed under a Creative Commons Attribution 4.0 International License.

[Read Full License](#)

---

# Abstract

## Purpose

The ability of plants to redistribute and transfer phosphorus (P) fractions determines their adaptability to P limitation. However, the mechanisms of P utilization and transport remain unknown in Chinese fir (*Cunninghamia lanceolata* (Lamb.) Hook.) from the perspective of P fraction distribution.

## Methods

In this study, we investigated the distribution and translocation patterns of total P and different P fractions in the M1 Chinese fir genotype, which has high P-use efficiency (PUE), using  $^{32}\text{P}$  tracking that can accurately trace the migration pathways of exogenous P after plant absorption.

## Results

We found that total P in roots was higher than in stems or leaves under P limitation when the amount of exogenous P absorbed by M1 reduced significantly. Under low-P, plants optimized P allocation, which led to higher PUE than under high-P, with the highest PUE in leaves, followed by stems and roots. The M1 genotype maintained a high ratio of soluble P (i.e., inorganic-P and ester-P) in its leaves and stems that increase P mobility and recycling under P limitation. In roots, P content shifted from soluble inorganic-P and ester-P to insoluble P (i.e., nucleic-P), but total P concentration was relatively stable, which may ensure root growth and exogenous P absorption under P limitation.

## Conclusion

Our results confirm the high PUE of the M1 genotype, which reduces P demand, maintains aboveground productivity, and optimizes the allocation of P among P fractions in response to P-limitation.

## Introduction

Plant nutritional acquisition strategies and their underlying mechanisms have long been a fundamental topic in ecology (Lambers et al. 2011). Phosphorus (P) is one of six macronutrients essential for plant growth and development due to its function in genetic material, free nucleotides for energy transfer, phospholipids as membrane components, and carbon metabolism as sugar phosphates (Ragothama and Karthikeyan 2005). However, P is a common limiting nutrient of productivity in forest species (Fink et al. 2014) due to its low soil mobility and precipitation with other soil minerals, such as iron (Fe) and aluminium (Al) in acidic soils and calcium (Ca) in alkaline soils (Bortoluzzi et al. 2015; Freitas et al. 2017). The development of forest cultivars with greater P use efficiency (PUE), defined as the ability to

grow and yield in soils with reduced P availability, would substantially improve forestry development (Lynch 2014).

P utilization in plants is affected by a series of physiological, structural, and growth characteristics (Huang et al. 2011). Under low P stress, plants can increase PUE by reducing metabolic activities and increasing P reuse (Hammond et al. 2009). Plants can accumulate both organic and inorganic P; inorganic P is composed of metabolic P and stored P (Rouached et al. 2011), while organic P can be divided between nucleic, ester, and lipid P (Kulmann et al. 2021; Piccin et al. 2017). Ester P and some inorganic P are actively metabolized by plant cells and are easily soluble, and the decomposition of ester P in cells is fundamental to energy and material metabolism. To some extent, the content of nucleic P can reflect the activity of plant protein synthesis and metabolism (Elser and Bennett 2011). Lipid P is insoluble and mainly forms the structural material of cell membranes (Hidaka and Kitayama 2011). Low P stress causes significant decreases in plant total P content and great variation in P distributions between tissues (Veneklaas et al. 2012). Plant species differ in the degree to which they can adjust the content and ratios of different P fractions to improve PUE (Shi et al. 2008). Lineages with high PUE tend to reduce insoluble and less-soluble P fractions while increasing the proportion of soluble inorganic P to enhance P mobility (Wieneke 1990). The contents and distribution of P fractions in plant tissues may also be affected by plant P nutritional status. P deficiency generally decreases the content and proportion of inorganic P more than organic P, which becomes the main P pool (Veneklaas et al. 2012; Liu et al. 2016; Shi et al. 2008).

Chinese fir (*Cunninghamia lanceolata* (Lamb.) Hook.) is a major species used for afforestation in southern China, but continuous planting and decreased soil fertility has caused reduced productivity and attracted the attention of many research groups. The low soil available P content resulting from strong P fixation in acidic soils is an important factor contributing to reductions in productivity (Fan et al. 2003). Recent studies of Chinese fir response to low-P stress (Chen et al. 2021; Lai et al. 2018; Zou et al. 2018) have identified genotypes with high PUEs (Wu et al. 2011). For example, the M1 genotype had high yields despite low soil P concentration relative to the average genotype (Xianhua et al. 2018). The mechanism underlying M1's high PUE has been confirmed to be P transport and reuse that accelerate the P-cycle: after inhibiting GA3 and IAA (Zou et al. 2019) in root tips and promoting the dissolution of root cortex to form aerenchyma (Wu et al. 2018), cellular P is transported to stems and leaves for reuse. Furthermore, insoluble rhizosphere P is activated through plant secretions (i.e., H<sup>+</sup>, total acid, oxalic acid, citric acid, etc.) (Lai et al. 2018; Zou et al. 2018) and apoptosis of root cells (Wu et al. 2017), thus improving P absorption efficiency. The ability of plants to redistribute and transfer P fractions affects their adaptability to P limitation (Guilbeault-Mayers et al. 2020; Moro et al. 2021). Few studies have tracked the distribution and translocation of P fractions in woody plants in multiple organs over time, although many have focused on leaves responses or herbaceous plants (Hidaka and Kitayama 2011; Guilbeault-Mayers et al. 2020; Wang et al. 2019). Thus, the mechanisms of P utilization and transport remain unknown in M1 Chinese firs from the perspective of P fraction distribution.

Here, we investigated the distribution and translocation of different P fractions in the M1 Chinese fir genotype with high P use efficiency after exogenous P uptake under low P supply. We used  $^{32}\text{P}$  labelling to assess short-term uptake of P because it can accurately trace the migration pathways of exogenous P after absorption into the plant. In brief, the method uses radioactive tracers to monitor the passage of nutrients through various plant tissues. Radioactive tracers have long been used to study nutrient translocation from soil to plant tissues (Feike et al. 2015; Mildaryani et al. 2020), because they provide reliable availability indices and correlate with measurements of chemical extraction. We chemically fractionated plant P into the following major fractions: inorganic P, and three classes of organic P (lipid, nucleic, and ester). We measured P at four times (0.5d, 1d, 5d, and 15d) to capture the dynamics of total P and P fractions in multiple organs under different levels of P supply. We then calculated the PUE of multiple organs and examined the relationships among different P fractions and PUE. We aimed to comprehensively explore P utilization in M1 Chinese firs from the perspective of P fraction distribution and translocation to identify mechanisms underlying increased PUE and provide a new empirical basis for the breeding of P use efficient plant genotypes.

## Materials And Methods

### Plant material

We used No.1 (M1) Chinese fir (*Cunninghamia lanceolata* (Lamb.) Hook.) seedlings that were identified in a preliminary study as exhibiting “passive low-P tolerance” that produced high yields despite low soil P concentration relative to the average genotype (Wu et al. 2011). Seedlings used in this study were half-sibs produced in monoculture from the Chinese fir clonal seed orchard at Wuyi State-owned Forest Farm, Zhangping, in Fujian Province, People’s Republic of China, which was established in 1985. Seedlings were cultivated in a greenhouse at the College of Forestry, Fujian Agriculture and Forestry University, People’s Republic of China, with an average temperature of 20.3°C and relative humidity was 78%. Seedlings were watered 3–4 times weekly. Seedlings had relatively consistent growth rates, complete root system, and showed no signs of disease. The average stem diameter at ground level was 2.30 mm and the average plant height was 17.00 cm.

### Study Design

The experiment was conducted in the Isotope Laboratory of the College of Sciences, Nanjing Agricultural University. Plants were grown in polyethylene containers (4.5cm diameter, 30cm depth) in hydroponic culture to ensure full absorption of exogenous P. Each seedling was wrapped with a sponge and fixed at the mouth of the container in a poly-ethylene foam plate with a 2cm diameter seedling hole cut in the middle of the foam plate. The stem-root transition zone of each seedling was wrapped in sponges and fixed in the seedling hole. During the experiment, a 20-min ventilation controlled by an automatic timer was performed every 4 h to ensure a sufficient oxygen supply to the seedlings.

Seedlings were divided between two P concentration conditions: high-P and low-P, with P concentrations set according to the soil available P in southern Chinese fir plantation forests measured by Sheng and Fan (2005), who showed that optimum available P in southern Chinese fir forests was 0.42 mmol/L (high-P) and the limiting value was 0.03 mmol/L (low-P). We used  $\text{KH}_2\text{PO}_4$  as the source of P, and high- and low-P treatments were  $0.50 \text{ mmol}\cdot\text{L}^{-1} \text{ KH}_2\text{PO}_4$  and  $0.03 \text{ mmol}\cdot\text{L}^{-1} \text{ KH}_2\text{PO}_4$ , respectively. The potassium (K) levels of the nutrient solutions used in the different treatments were adjusted with KCl during the experiment based on the modified Hoagland formula of Wu et al. (2011):  $127.5 \text{ mg}\cdot\text{L}^{-1} \text{ KNO}_3$ ,  $122.5 \text{ mg}\cdot\text{L}^{-1} \text{ MgSO}_4\cdot 7\text{H}_2\text{O}$ ,  $294.92 \text{ mg}\cdot\text{L}^{-1} \text{ Ca}(\text{NO}_3)_2\cdot 4\text{H}_2\text{O}$ , trace elements ( $0.71 \text{ mg}\cdot\text{L}^{-1} \text{ H}_3\text{BO}_3$ ,  $0.02 \text{ mg}\cdot\text{L}^{-1} \text{ CuSO}_4\cdot 5\text{H}_2\text{O}$ ,  $0.055 \text{ mg}\cdot\text{L}^{-1} \text{ ZnSO}_4\cdot 7\text{H}_2\text{O}$ ,  $0.4525 \text{ mg}\cdot\text{L}^{-1} \text{ MnCl}_2\cdot 4\text{H}_2\text{O}$ , and  $0.015 \text{ mg}\cdot\text{L}^{-1} \text{ H}_2\text{MO}_4\cdot 4\text{H}_2\text{O}$ ), and an iron salt solution ( $1.393 \text{ mg}\cdot\text{L}^{-1} \text{ FeSO}_4\cdot 7\text{H}_2\text{O}$  and  $1.863 \text{ mg}\cdot\text{L}^{-1} \text{ Na}_2\text{EDTA}$ ). The pH of the nutrient solution was adjusted to 5.5 with NaOH and diluted HCl.

$^{32}\text{P}$  is an ideal radionuclide for use in plant physiology and fertilization studies due to its nuclear features: it is a pure beta emitter with the maximum  $\beta^-$  radiation energy  $E_{\text{max}}=1.7 \text{ MeV}$  and a half-life of 14.3d. Based on these properties, we assessed plant P at four times during the experiment (0.5d, 1d, 5d, and 15d). We prepared the  $^{32}\text{P}$  radioactive solution using a stock solution of  $^{32}\text{P}$ -orthophosphate with a radioactive concentration of  $4.05\times 10^4 \text{ Bq}\cdot\text{mL}^{-1}$  (PerkinElmer, U.S). Each single seedling pot contained 250 mL nutrient solution and 650  $\mu\text{L}$  of  $^{32}\text{P}$ -orthophosphate solution, and there were five replicates for each treatment, for a total of 40 seedlings. We also prepared five polyethylene containers without seedlings for each nutrient solution (i.e., high- and low-P concentrations) and  $^{32}\text{P}$ -orthophosphate solution, which were used as blanks to determine the specific activity at the end of the experiment.

## Determination Of Indicators

### Determination of dry weight

After each P treatment, the nutrient solution was washed from the root surface of seedlings with deionized water until the radioactivity of  $^{32}\text{P}$  on the root surface was less than 100 counts per minute (cpm), as determined by a liquid scintillation counter (LSC; Beckman LS6500). Then fresh leaf, stem, and root of Chinese fir seedlings were separated and oven-dried at  $105^\circ\text{C}$  for 2 h and then at  $75^\circ\text{C}$  to constant mass to determine dry mass (DM). Before oven-drying, small fresh samples of each organ were taken and stored at  $-80^\circ\text{C}$  for the determination of radioactivity (below).

### Determination of radioactivity

#### Radioactivity determination of total P and different P fractions in seedlings

For each plant, 0.03g crushed samples of each organ (root, stem, and leaf) were weighed for radioactivity determination of total P. We also separately weighed 0.20g fresh samples of root, stem, and leaf, ground them into homogenates, and rinsed them with 4 mL of 5% trichloroacetic acid (TCA) in centrifuge tubes. Then 1 mL 5% TCA was added and samples were centrifuged at  $1180\times g$  for 5 minutes. We transferred

the resulting supernatants into 25mL volumetric flasks, added 5mL acetone, shook well, added 5mL ammonium molybdate reagent, mixed, let rest for a few minutes, and then them transferred into a separatory funnel. We then added 10mL of a water-saturated mixture of isobutanol and benzene to each sample and vigorously shook. After resting for a few minutes, the solutions separated into two layers: an acidic inorganic P (Pi) bottom layer and organic P compound upper layer. We collected the two layers in 25mL volumetric flasks containing distilled water for Pi and acetone for organic P. After the main component of the organic P solution (ester P) was removed, we extracted the residue with 3 mL of 95% (w/v) ethanol. We continued to extract with a total of 3mL 2:1 mixed solution (ethanol and ether, v/v) after resting the solution for 10 minutes and centrifuging at 1089×g for 8 minutes. Each extraction resulted in a lipid P supernatant and the extraction solution was adjusted to 25ml with acetone. The precipitate was hydrolyzed with 5mL of 0.5mol KOH at 36°C for 18h, cooled, MgCl<sub>2</sub> was added to accelerate RNA decomposition, and acidified to pH = 1 with 72% HClO<sub>4</sub> before centrifuging at 1180×g for 10 minutes. The resulting supernatant contained <sup>32</sup>P-RNA, and the volume was fixed to 25 ml with distilled water. A final precipitate was extracted by adding 5 mL 5% HClO<sub>4</sub> and incubating at 90°C in a water bath for 15 minutes. The solution was separated into two layers after centrifuging at 1180×g for 10 minutes, and a supernatant containing <sup>32</sup>P-DNA was extracted and brought to 25 ml with distilled water.

The above extraction steps were repeated four times for complete separation, and final P fractions were determined uniformly. All samples were decolorized and filtered with activated carbon, then 1mL was pipetted, and the radioactivity of the samples was determined by liquid scintillation counter (Beckman LS6500) after adding scintillation liquid (PerkinElmer, Boston,U.S) for 12h. Data obtained from LSC were transformed into units of disintegration per minute (dpm) by dividing cpm by LSC efficiency: dpm = cpm/efficiency (Nurmayulis et al. 2013). Data was recorded as the average of five replications. The reference moment chosen for all activity results was the harvesting time. <sup>32</sup>P uptake was calculated using the following decay correction.

$$A = A_0 e^{-\lambda t}$$

1

Where  $A$  is the remaining activity of <sup>32</sup>P after decay at time  $t$  (from the measurement time to the reference time),  $A_0$  is the activity of <sup>32</sup>P at  $t=0$ , and  $\lambda$  is the decay constant of <sup>32</sup>P. The formula for calculating  $\lambda$  is  $\lambda = \ln 2 / T_{1/2}$ , where  $T_{1/2}$  is the half-life of <sup>32</sup>P, which is 14.3d.

Determination of activity specific

Specific activity, expressed in units of Bq·μg<sup>-1</sup>, was defined as the ratio of radioactivity to P content in the five blank solutions (see Study Design, above) and calculated as follows:

$$SA = \frac{R_l}{m_p} \quad (2)$$

Where SA is specific activity,  $R_i$  is the radioactivity of nutrient solution, and  $m_p$  is P content in nutrient solution.

### Data Analyses

We calculated the content of exogenous P of each organ on a dry matter basis by dividing the radioactivity of each organ by the specific activity and dry mass:

$$M_{TP} = \frac{R_{TP} * \frac{1}{SA}}{m_0}$$

3

Where  $M_{TP}$  (expressed in units of  $\mu\text{g}\cdot\text{g}^{-1}$ ) is the content of exogenous P of each organ on a dry matter basis,  $R_{TP}$  (expressed in units of Bq) is the radioactivity of total P in each organ, SA (expressed in units of  $\text{Bq}\cdot\mu\text{g}^{-1}$ ) is the specific activity (Eq. 2), and  $m_0$  (expressed in units of g) is dry mass of each organ. Eq. 3 was also used to calculate the content of each P fraction in each organ was calculated similarly.

We also calculated the distribution ratio of different P fractions in each organ to total plant P; the distribution ratios ( $r_{FP}$ , %) was calculated as follows:

$$r_{FP} = \frac{M_{FP}}{M} * 100\% \quad (4)$$

Where  $r_{FP}$  is distribution ratio of a given P fraction in a given each organ,  $M_{FP}$  is the content of that P fraction in the organ on a dry matter basis, and M (expressed in units of  $\mu\text{g}\cdot\text{g}^{-1}$ ) is the sum of  $M_{TP}$  in different organs.

Finally, we calculated the P use efficiency (PUE,  $\text{g}\cdot\mu\text{g}^{-1}$ ) of each organ, to investigate the rate of dry mass synthesis per unit P in each organ:

$$\text{PUE} = \frac{m_0}{m_0 * M_{TP}}$$

5

Statistical analyses were performed in SPSS version 19.0 (SPSS Inc., Chicago, IL, U.S), and graphs were plotted using Origin 8.5 (Origin Lab Corporation, Northampton, MA, U.S). Paired t-tests were used to compare differences between high and low P treatments at each time point. One-way ANOVA was used to evaluate differences between time points for total P concentrations, distribution ratios, relative proportions of each P fraction, and PUE. Pearson correlation analysis was used to examine the relationships among different P fractions and PUE. All tests were done using a confidence level of  $P <$

0.05. We further investigated significant effects with Duncan's multiple range test at 5% significance level to test for differences between treatments.

## Results

### Comparison of total P distributions after different P treatments

The amount of exogenous P absorbed by plants under both high and low P treatments increased gradually with time (Fig. 1). The distribution of exogenous P in roots was significantly higher than that in leaves and stems. The amount of exogenous P in leaves and stems only reached 7.7%-10.5% of that in roots under different P supply conditions after 15 days, when the absorption curves of exogenous P in leaves and stems showed no significant difference between them. Comparison of the high- and low-P treatments showed that the amount of exogenous P absorbed by plants under low-P treatment was significantly lower than that of the high-P treatment ( $P < 0.05$ ). The differences were initially quite small, but P uptake in high-P treatment increased sharply from 5d to 15d. The amount of exogenous P absorbed by roots under low-P treatment at 5d and 15d was only 13.3% and 4.8% of that of high-P condition, respectively.

Ratios of exogenous P absorbed in different organs showed that root absorbed the most exogenous P (80%-90%), followed by stems and leaves, regardless of P treatment (Fig. 2). The ratio of exogenous P in aboveground parts initially decreased over the first day but increased in both treatments over 5d and 15d. The ratios of root, stem, and leaf P were similar in the high- and low-P treatments at 0.5d ( $P > 0.05$ ), but leaf and stem P ratios decreased under low-P treatment relative to the high-P treatment ( $P < 0.05$ ). The ratios of stem P under low-P were 59.4% and 75.2% of high-P treatment after 5d and 15d. In leaves the ratios were similarly low; only 43.2% and 73.9% of the high-P treatment at 5d and 15d, respectively. In contrast, the ratio of P in roots was higher under low-P treatment than high-P supply from 1d to 15d.

### Distribution of P fractions in leaves under different P treatments

The content of P fractions at 0.5d in leaves under both conditions were lower than the detection limit, which we recorded them as  $0 \mu\text{g}\cdot\text{g}^{-1}$  (Fig. 3). We found that the distributions of inorganic-P and ester-P in leaves were similar between high- and low-P treatments. Under high-P supply, the ratios of inorganic-P and ester-P peaked at 5d before decreasing significantly at 15d ( $P > 0.05$ ; Fig. 3a-b). Under low-P treatment, the ratios of inorganic-P and ester-P in leaves increased over the experiment, and the ratios after 15d were significantly higher than all earlier time points ( $P > 0.05$ ; Fig. 3a-b), and both were higher than those of the high-P treatment. The ratio of soluble P remained high in leaves of M1 Chinese fir under low-P treatment. The lipid-P in leaves increased over 5d in both high- and low-P conditions and remained stable between 5d and 15d (Fig. 3c). The ratios of lipid-P under low-P treatment decreased relative to the high-P treatment ( $P < 0.05$ ) at 5d and 15d, when the ratio was significantly lower than high-P treatment at 1d ( $P < 0.05$ ). Similarly, the ratio of nucleic P in leaves increased up to 5d and remained stable from 5d to 15d under high P supply, while the proportion of nucleic P in leaves increased continuously under low P

treatment (Fig. 3d). In the low-P treatment, the nucleic-P ratio at 15d reached 4 times that of 1d and was significantly higher than that under high-P supply ( $P < 0.05$ ).

#### Distribution of P fractions in stems under different P treatments

As in leaves, stem P fractions at 0.5d were below the detection limit and recorded as  $0 \mu\text{g}\cdot\text{g}^{-1}$  (Fig. 4). The distribution of inorganic-P and ester-P in stems was consistent with that observed in leaves: ratios peaked at 5d under high-P supply but increased over the course of the experiment under low-P (Fig. 4a-b). The ratios of inorganic-P and ester-P were also higher under low-P treatment at 15d, with the ratio of inorganic-P under low-P twice that of high-P. The ratio of soluble P in M1 stems also remained high under low-P treatment. Like leaves, there was no significant difference between lipid-P ratios in stems of different P treatments ( $P \geq 0.05$ ), but lipid-P increased slightly by 15d under low-P treatment (Fig. 4c). The ratio of nucleic-P in stems was also consistent with that in leaves: the ratio of nucleic-P in stems increased up to 5d and was stable from 5d to 15d under high-P supply, while the proportion of nucleic-P in stems continuously significantly increased under low-P supply (Fig. 4d).

#### Distribution of P fractions in roots under different P treatments

The changes in inorganic-P and ester-P in roots were different from trends in leaves and stems. Regardless of P supply treatment, inorganic-P in root generally decreased over the course of the experiment (Fig. 5a), while ester-P peaked at 1d and was not significantly different between 0.5d, 5d, and 15d (Fig. 5b). The ratios inorganic-P and ester-P were also lower under low-P treatment than high-P supply from 0.5d to 15d, and the differences at most time points were significant ( $P \leq 0.05$ ; Fig. 5a-5b). We did not observe any changes in the ratios of lipid-P in roots of either P treatment ( $P \geq 0.05$ ; Fig. 5c), but lipid-P was slightly slowed in the low P treatment. The patterns of root nucleic-P ratios were markedly different between high and low P treatments. Under high-P supply, the ratio of nucleic-P was constant over time ( $P \geq 0.05$ ), while the ratio of nucleic-P increased significantly with time under low-P treatment (Fig. 5d). The ratio of nucleic-P in roots at 15d was 2.6 times that of 0.5d under low-P treatment. Moreover, in contrast to root inorganic-P, ester-P, and lipid-P, all ratios of nucleic-P were higher in the low-P treatment than high-P supply over the course of the experiment.

#### P use efficiency in different organs under different P treatments

The P use efficiency (PUE) was highest in each organ at 0.5d ( $P < 0.05$ ) under both high- and low-P treatments (Fig. 6). PUE of each organ from reduced slightly from 1d to 15d under low-P treatment, but there was no significant difference between time points ( $P \geq 0.05$ ). The PUEs of leaves, stems, and roots at 15d under low-P treatment were only 1.53%, 1.57%, and 1.27% of that at 0.5d, respectively. Similarly, under high-P, PUE of each organ decreased from 0.5d to 1d and then remained stable. Leaf PUE was highest, followed by stem and root, regardless of P treatment. The PUE of leaves was nearly 9 times that of roots at 0.5d under low-P treatment, and reached more than 10 times under high-P treatment. Comparison of high- and low-P treatments at each time point showed that the PUE of each organ under low-P was significantly higher than under high-P at each time point ( $P < 0.05$ ). For example, the PUEs of

leaves, stems, and roots at 0.5d under high-P were only 6.90%, 6.24%, and 5.70% of that under low-P, respectively.

### Relationship between P fractions and PUE in different organs

Correlation analysis between different P fractions and PUE showed that the PUEs of leaves and stems were both similarly negatively correlated with each P fraction, regardless of P treatment (Table 1). Furthermore, leaf PUE was significantly negatively correlated ( $P < 0.01$ ) with inorganic-P, ester-P, and nucleic-P under low-P treatment. The correlations between PUE and these three fractions in stems were also significant ( $P < 0.05$ ). However, the correlations between PUE and P fractions in leaves and stems were not significant ( $P > 0.05$ ) under high-P, except for ester-P. In roots, PUE was significantly negatively correlated with nucleic-P ( $P < 0.01$ ) under low-P and significantly negatively correlated with ester-P under high-P ( $P < 0.05$ ).

Table 1  
Correlations between P fractions and PUE in different organs

P fractions	PUE for dry mass ( $\text{g} \cdot \mu\text{g}^{-1}$ )					
	Leaf		Stem		Root	
	L-P	H-P	L-P	H-P	L-P	H-P
Inorganic-P	-0.990 <sup>**</sup>	-0.734 <sup>ns</sup>	-0.798 <sup>*</sup>	-0.701 <sup>ns</sup>	-0.018 <sup>ns</sup>	0.661 <sup>ns</sup>
Ester-P	-0.980 <sup>**</sup>	-0.858 <sup>*</sup>	-0.816 <sup>*</sup>	-0.607 <sup>ns</sup>	0.056 <sup>ns</sup>	-0.796 <sup>*</sup>
Lipid-P	-0.720 <sup>ns</sup>	-0.772 <sup>ns</sup>	-0.642 <sup>ns</sup>	-0.723 <sup>ns</sup>	0.440 <sup>ns</sup>	-0.623 <sup>ns</sup>
Nucleic-P	-0.940 <sup>**</sup>	-0.767 <sup>ns</sup>	-0.813 <sup>*</sup>	-0.785 <sup>ns</sup>	-0.878 <sup>**</sup>	-0.549 <sup>ns</sup>

<sup>ns</sup> represent not significant with  $P > 0.05$ , <sup>\*</sup> represent significant differences at  $P < 0.05$ , <sup>\*\*</sup> represent significant differences at  $P < 0.01$ ; PUE represent P use efficiency, L-P and H-P represent the low-P and high-P treatment, respectively.

## Discussion

P is among the most intractable constraints on plant fertility, particularly in acidic soils in the tropics with high P fixation capacities. The effects of nutrient limitation and plant adaptive strategies in infertile soils is a focal topic of plant ecology. Plants can adjust the content and ratios of P fractions to improve nutrient utilization efficiency (Shi et al. 2008). We found that the amount of exogenous P absorbed by the M1 genotype of Chinese fir decreased significantly under low-P treatment, and that total P in root was significantly higher than in shoot. Congruent with recent studies of foliar P fractions (Hidaka et al. 2013), M1 Chinese firs generally reduced total and leaf P concentrations. This decrease in total P concentration is caused by the reduction of P fractions in cells and various P-containing biochemical compounds (Hidaka and Kitayama 2011; Veneklaas et al. 2012), and plants optimize P allocation among foliar P

fractions to increase P use efficiency (PUE) under low soil P availability (Hidaka et al. 2013). Our results are congruent with the past reports: PUE under low-P treatment was generally significantly higher than under high-P across time points and plant organs. Furthermore, the PUE of leaves and stems were significantly negatively correlated with inorganic-P, ester-P, and nucleic-P under low-P treatment, while root PUE was significantly negatively correlated with nucleic-P.

We also observed that the M1 Chinese fir genotype optimized P allocation among foliar P fractions under low soil P availability. It has been widely reported that plants generally reduce foliar P concentration and enhance PUE in response to low soil P availability (Nadejda et al. 2007; Hidaka and Kitayama 2010; Yan et al. 2015; Yang et al. 2018). An analysis of 340 tree and shrub species across various biomes found that plants growing in P-poor soils increased leaf toughness and leaf life span, thus allowing a greater P fraction to be allocated for metabolism rather than growth to maintain high PUE (Hidaka and Kitayama 2011). M1 Chinese fir optimize P allocation (i.e., enhancing PUE) to maintaining productivity and growth and reduce P demand (i.e., reduce total P concentration) under limiting P conditions. Furthermore, increased PUE could be explained by the net effect of a relatively greater investment of P into Pi and P-containing metabolites for growth and less into other foliar P fractions (i.e., membrane phospholipids) in addition to generally reduced concentrations of all P fractions (Hidaka and Kitayama 2013).

In this study, we found that PUE was highest in leaves, followed by stems and roots, and the leaf PUE was significantly correlated with inorganic-P, ester-P, and nucleic-P under low-P treatment. Previous studies have shown that inorganic-P is expected to have higher resorption efficiency due to its high mobility (Tsuji et al. 2017). In contrast, much more energy is required to degrade recalcitrant P compounds in senesced leaves to increase P resorption efficiency in P-limited environments (Hidaka and Kitayama 2013). Our results showed that the ratio of soluble P (i.e., inorganic-P and ester-P) remained high in leaves of M1 Chinese firs under low-P treatment while lipid-P was lower, relative to the high-P treatment. The proportion of nucleic-P in leaves also gradually increased under low-P treatment, which may potentially limit growth and productivity (Tsuji et al. 2017), similar to inorganic-P. These findings are generally consistent with previous studies, which showed a relatively greater investment of P into inorganic P and P-containing metabolites. Lipid-P showed lower content under high P supply, while the proportion of soluble P in stems likely increased P mobility and improved the P recycling capacity of P (Mo et al. 2019; Liu et al. 2016; Shi et al. 2008).

In contrast to shoot and leaf patterns, inorganic-P in roots decreased over the course of the experiment and ester-P peaked at 1d in both treatment groups. Root nucleic P was constant under high-P but increased significantly with time under low-P treatment. Studies of ecological stoichiometry have suggested that a great amount of nucleic-P is in P-rich ribosomal RNA and that higher rates of plant growth required a greater investment in ribosomal RNA to produce the proteins required for growth (Perkins et al. 2004). These findings suggest that an increase in protein synthesis requires higher P allocation to nucleic-P; thus, higher root nucleic-P may be a response to promote root growth to improve exogenous P absorption under P-limitation. However, soluble P content gradually decreased relative to insoluble P components under P-limitation. We speculate that P fractions in roots were transferred. Plant

absorption of P is strongly limited by exogenous P, which ultimately limits plant growth (Yuan and Chen 2015). To satisfy P demand for shoots, plants take up nutrients from the soil but also recycle nutrients internally through resorption and re-allocation from storage organs (e.g., roots), which allows the reuse of nutrients for new growth ( Klimeová et al. 2018; Valverde-Barrantes et al. 2017; Wang et al. 2021). A study by Lambers found that P resorption efficiency (from Pi and P mobilized from hydrolyzed lipids and nucleic acids prior to abscission) approached 82% on sites with severe P deficiency (2015). Other studies have shown that under low P stress, high P efficient plants enhance the decomposition of ester-P and nucleic-P by increasing the activity of acid phosphatase in lower leaves so that newer, upper leaves can reuse their P (Liu et al. 2016). It has been hypothesized that the ability of plants to redistribute and transfer P fractions affects their adaptability to P limitation (Mo et al. 2019; Hidaka and Kitayama 2013; Wang et al. 2019).

Previous studies of P fractions have focused exclusively on leaf responses or herbaceous plants (Hidaka and Kitayama 2011; Guilbeault-Mayers et al. 2020; Wang et al. 2019). Few studies have tracked the distribution and translocation of P fractions in woody plants in multiple organs over time. Species vary in their P absorption and utilization strategies, which is reflected in the distribution of P fractions (Mo et al. 2019; Tsujii et al. 2017). Here, we observed the dynamics of P fractions in M1 Chinese firs under low P condition using highly precise  $^{32}\text{P}$  isotope tracer techniques. Our findings were generally consistent with earlier studies that found relatively greater P allocation to Pi and P-containing metabolites in leaves and shoots. Our results support the hypothesis that higher shoot soluble P enhances P mobility and recycling. In contrast, we observed large increases in nucleic-P in root, which are generally analyzed from the perspective of a storage organ. We believe that the M1 Chinese fir genotype has high P-use efficiency, which reduces P demand, maintains aboveground productivity, and increases root nutrient allocation in response to P-limitation.

## Conclusion

We found that under limiting P, the M1 Chinese fir genotype reduced the allocation of exogenous P to leaves and stems, and correspondingly increased the distribution to roots, in addition to generally reducing total P concentrations. However, the PUE of different organs under low-P were all significantly higher than under high-P treatment over the course of the experiment. PUE was generally significantly correlated with P fractions (i.e., inorganic-P, ester-P, and nucleic-P), which showed that higher PUE under low-P was explained by the net effect of a relatively greater investment of P into metabolic P rather than to structural P. M1 Chinese firs maintained a high ratio of soluble P (inorganic-P and ester-P) in leaves and stems to increase P reuse capacity to adapt to low soil P availability. Our results suggest that P is transferred in roots, as soluble inorganic-P and ester-P gradually decreased while insoluble P components (e.g., nucleic-P) accumulated in the roots to maintain a relatively stable root total P concentration. These responses likely facilitate root growth to increase exogenous P absorption under low P supply. We conclude that M1 Chinese fir genotype has high PUE, which reduces P demand (i.e., reduces total P

concentration), maintains aboveground productivity (i.e., increases PUE), and optimizes the allocation of P among P fractions (i.e., increases P mobility and recycling) in response to P-limitation.

## Declarations

### Funding

This work was supported by the National Natural Science Foundation of China (Grant No. 32160361) and the Natural Science Foundation of Fujian Province (Grant No. 2020J01519).

### Competing Interests

The authors have no relevant financial or non-financial interests to disclose.

### Author Contributions

Xianhua Zou contributed to the study conception and design. Xiangqing Ma and Pengfei Wu helped in conducting the experiments and data analysis. Sitong Chen set up the experiment, prepared the seedlings and performed laboratory works. Qingqing Liu and Zhijun Huang contributed to data collection and analysis. The first draft of the manuscript was written by Xianhua Zou with suggestions from all the coauthors. All authors contributed critically to the drafts and gave final approval for publication.

### Data Availability

We conform that, should the manuscript be accepted, the data DOI will be included at the end of the article.

## References

1. Bortoluzzi EC, Pérez CAS, Ardisson JD, Tiecher T, Caner L (2015) Occurrence of iron and aluminum sesquioxides and their implications for the phosphorus sorption in subtropical soils. *Appl Clay Sci* 104: 196-204. <https://doi.org/10.1016/j.clay.2014.11.032>
2. Chen W, Zhou M, Zhao M, Chen R, Ma X (2021) Transcriptome analysis provides insights into the root response of Chinese fir to phosphorus deficiency. *BMC Plant Biol* 21:525. <https://doi.org/21203/rs.3.rs-400319/v1>
3. Elser J, Bennett E (2011) Phosphorus cycle: A broken biogeochemical cycle. *Nature* 478:29-31. <https://doi.org/10.1038/478029a>
4. Fan S, Shen W, Ma X, Lin K, Zhang X (2003) Effect of successive planting on productivity of Chinese fir of different age plantations. *Forest Res* 16:560-567. <https://doi.org/10.3321/j.issn:1001-1498.2003.0007>
5. Feike AD, He M, Johansen MP, Jennifer JH, Claudia K (2015) Plant and microbial uptake of nitrogen and phosphorus affected by drought using  $^{15}\text{N}$  and  $^{32}\text{P}$  tracers. *Soil Biol Biochem* 82:135-142.

<https://doi.org/10.1016/j.soilbio.2014.12.021>

6. Fink JR, Inda AV, Bayer C, Torrent J, Barrón V (2014) Mineralogy and phosphorus adsorption in soils of south and central-west Brazil under conventional and no-tillage systems. *Acta Sci Agron* 36:379-387. <https://doi.org/10.4025/actasciagron.v36i3.17937>
7. Freitas ECSD, Paiva HND, Leite HG, Oliveira N (2017) Effect of phosphate fertilization and base saturation of substrate on the seedlings growth and quality of *Plathymenia foliolosa*. *Rev Árvore* 41: e410111. <http://dx.doi.org/10.1590/1806-90882017000100011>
8. Hammond JP, Broadley MR, White PJ, King GJ, Bowen HC, Hayden R, Meacham MC, Mead A, Overs T, Spracklen W P (2009) Shoot yield drives phosphorus use efficiency in Brassica oleracea and correlates with root architecture traits. *J Exp Bot* 60:1953-1968. <https://doi.org/10.1093/jxb/erp083>
9. Hidaka A, Kitayama K (2011) Allocation of foliar phosphorus fractions and leaf traits of tropical tree species in response to decreased soil phosphorus availability on Mount Kinabalu, Borneo. *J Ecol* 99: 849-857. <https://doi.org/10.1111/j.1365-2745.2011.01805.x>
10. Hidaka A, Kitayama K (2013) Relationship between photosynthetic P-use efficiency and foliar phosphorus fractions in tropical tree species. *Ecol Evol* 3: 4872-4880. <https://doi.org/10.1002/ece3.861>
11. Hidaka A, Kitayama K (2010) Divergent patterns of photosynthetic phosphorus-use efficiency versus nitrogen-use efficiency of tree leaves along nutrient-availability gradients. *J Ecol* 97:984-991. <https://doi.org/10.1111/j.1365-2745.2009.01540.x>
12. Hidaka K, Dan K, Imamura H, Miyoshi Y, Takayama T, Sameshima K, Kitano M, Okimura M (2013) Effect of supplemental lighting from different light sources on growth and yield of strawberry. *Environ Control Biol* 51: 41-47. <https://doi.org/10.2525/ecb.51.41>
13. Huang C, Shirley N, Genc Y, Shi B, Langridge P (2011) Phosphate utilization efficiency correlates with expression of low-affinity phosphate transporters and noncoding RNA, IPS1, in Barley. *Plant Physiol* 156:1217-1229. <https://doi.org/10.1104/pp.111.178459>
14. Klimeová M, Rindi F, Kaloud P (2018) There is more than meets the eye: DNA cloning demonstrates high genetic heterogeneity in populations of the subaerial green alga *Trentepohlia* (*Trentepohliales*, *Chlorophyta*). *J Phycol* 55:224-235. <https://doi.org/10.1111/jpy.12817>
15. Kulmann MSS, Stefanello LOS, Schwalbert RA, Berghetti LLP, Brunetto G (2021) Effects of phosphorus fertilizer application on phosphorus fractions in different organs of *Cordia trichotoma*. *J Forestry Res* 32:725-732. <https://doi.org/10.1007/s11676-020-01136-4>
16. Lai H, Wu K, Wang N, Wu W, Wu P (2018) Relationship between volatile organic compounds released and growth of *Cunninghamia lanceolata* roots under low-P conditions. *iForest* 11:713-720. <https://doi.org/10.3832/ifor2797-011>
17. Lambers H, Brundrett MC, Raven JA and Hopper SD (2011) Plant mineral nutrition in ancient landscapes: high plant species diversity on infertile soils is linked to functional diversity for nutritional strategies. *Plant Soil* 348:7-27. <https://doi.org/10.1007/s11104-011-0977-6>

18. Lambers H, Hayes PE, Laliberté E, Oliveira RS, Turner BL (2015) Leaf manganese accumulation and P-acquisition efficiency. *Trends Plant Sci* 20:83-90. <https://doi.org/10.1016/j.tplants.2014.10.007>
19. Liu T, Chen H, Yu H, Li T, Gao S (2016) Characterization of phosphorus utilization in Barley leaf under low phosphorus stress. *Chin Bull Bot* 51:504-514. <https://doi.org/10.11983/CBB16028>
20. Lynch JP (2014) Root phenes that reduce the metabolic costs of soil exploration: opportunities for 21st century agriculture. *Plant Cell Environ* 38:1775-1784. <https://doi.org/10.1111/pce.12451>
21. Guilbeault-Mayers X, Turner BL, Laliberté E (2020) Greater root phosphatase activity of tropical trees at low phosphorus despite strong variation among species. *Ecology* 101: e03090. <https://doi.org/10.1002/ecy.3090>
22. Mildaryani W, Mujiyo M, Dewi WS, Poernomo D (2020) Isotopic tracing of phosphorus uptake in Oil Palm seedlings leaf axil using  $^{32}\text{P}$  labelled. *Int J Adv Sci Eng Inf Tech* 10:368-373. <https://doi.org/10.18517/ijaseit.10.1.11119>
23. Mo Q, Li Z, Sayer EJ, Lambers H, Li Y, Zou B, Tang J, Heskell M, Ding Y, Wang F (2019) Foliar phosphorus fractions reveal how tropical plants maintain photosynthetic rates despite low soil phosphorus availability. *Funct Ecol* 33:503-513. <https://doi.org/10.1111/1365-2435.13252>
24. Moro H, Park HD, Kunito T (2021) Organic phosphorus substantially contributes to crop plant nutrition in soils with low phosphorus *Agronomy* 11:903. <https://doi.org/10.3390/agronomy11050903>
25. Nadejda A, Soudzilovskaia, Vladimir G, Onipchenko, Johannes HC, Cornelissen, Rien Aerts (2007) Effects of fertilisation and irrigation on 'foliar afterlife' in alpine tundra. *J Veg Sci* 18:755-766. <https://doi.org/10.1111/j.1654-1103.2007.tb02591.x>
26. Nurmayulis N, Citraesmini A, Anas I (2013) The use of  $^{32}\text{P}$  method to evaluate the growth of lowland rice cultivated in a system of rice intensification (SRI). *Atom Indonesia* 39:88. <https://doi.org/10.17146/aij.2013.236>
27. Perkins MC, Woods HA, Harrison JF, Elser JJ (2004) Dietary phosphorus affects the growth of larval *Manduca sexta*. *Arch Insect Biochem Physiol* 55:153-168. <https://doi.org/10.1002/arch.10133>
28. Piccin R, Couto RDR, Bellinaso RJS, Gatiboni LC, Conti LD, Rodrigues LAT, Michelon LS, Kulmann MSDS, Brunetto G (2017) Phosphorus forms in leaves and their relationships with must composition and yield in grapevines. *Pesquisa Agropecuária Brasileira* 52:319-327. <https://doi.org/10.1590/s0100-204x2017000500005>
29. Ragothama KG, Karthikeyan AS (2005) Phosphate acquisition. *Plant Soil* 274:37-49. [https://doi.org/10.1007/1-4020-4099-7\\_2](https://doi.org/10.1007/1-4020-4099-7_2)
30. Rouached H, Stefanovic A, Secco D, Arpat AB, Gout E, Bligny R, Poirier Y (2011) Uncoupling phosphate deficiency from its major effects on growth and transcriptome via *PHO1* expression in *Arabidopsis*. *Plant J* 65:557-570. <https://doi.org/10.1111/j.1365-313X.2010.04442.x>
31. Sheng W, Fan S (2005) Long-term productivity of Chinese fir plantations. Science Press, Beijing.

32. Shi L, Liang H, Xu F, Wang Y (2008) Genotypic variation in phosphorus fractions and its relation to phosphorus efficiency in seedlings of *Brassica napus* Plant Nutr Fert Sci 14:351-356. <https://doi.org/10.3321/j.issn:1008-505X.2008.02.023>
33. Tsujii Y, Onoda Y, Kitayama K (2017) Phosphorus and nitrogen resorption from different chemical fractions in senescing leaves of tropical tree species on Mount Kinabalu, Borneo. Oecologia 185:171-180. <https://doi.org/10.1007/s00442-017-3938-9>
34. Valverde-Barrantes OJ, Gregoire TF, Roumet C, Blackwood CB (2017) A worldview of root traits: the influence of ancestry, growth form, climate and mycorrhizal association on the functional trait variation of fine-root tissues in seed plants. New Phytol 215: 1295-  
<https://doi.org/10.1111/nph.14571>
35. Veneklaas EJ, Lambers H, Bragg J, Finnegan PM and Raven JA (2012) Opportunities for improving P-use efficiency in crop plants. New Phytol 195:306-320. <https://doi.org/10.1111/j.1469-8137.2012.04190.x>
36. Wang FC, Fang XM, Wang GG, Rong, Chen FS (2019) Effects of nutrient addition on foliar phosphorus fractions and their resorption in different-aged leaves of Chinese fir in subtropical China. Plant Soil 443:41-54. <https://doi.org/10.1007/s11104-019-04221-8>
37. Wang R, Cresswell T, Johansen MP, Harrison JJ, Jiang Y, Keitel C, Cavagnaro TR, Dijkstra FA (2021) Re-allocation of nitrogen and phosphorus from roots drives regrowth of grasses and sedges after defoliation under deficit irrigation and nitrogen enrichment. J Ecol 109:4071-4080. <https://doi.org/10.1111/1365-2745.13778>
38. Wieneke J (1990) Phosphorus efficiency and phosphorus remobilization in two sorghum (*Sorghum bicolor* (L.) Moench) cultivars. Plant Soil 123:139-145. [https://doi.org/10.1007/978-94-009-2053-8\\_10](https://doi.org/10.1007/978-94-009-2053-8_10)
39. Wu P, Lai H, Mulualet T, Wu W, Wang P, Wang G, Ma X (2018) Does phosphorus deficiency induce formation of root cortical aerenchyma maintaining growth of *Cunninghamia lanceolata*? Trees, 32:1633-1642. <https://doi.org/10.1007/s00468-018-1739-3>
40. Wu P, Ma X, Mulualet T, Wang C, Odén PC (2011) Root morphological plasticity and biomass production of two Chinese fir clones with high phosphorus efficiency under low phosphorus stress. Can J Forest Res 41:228-234. <https://doi.org/10.1139/X10-198>
41. Wu P, Wang G, El-Kassaby YA, Wang P, Zou X, Ma X (2017) Solubilization of aluminum-bound phosphorus by root cell walls: evidence from Chinese fir, *Cunninghamia lanceolata*. Can J Forest Res 47:419-423. <https://doi.org/10.1139/cjfr-2016-0310>
42. Yan K, Duan C, Fu D, Li J, Wong M, Qian L, Tian Y (2015) Leaf nitrogen and phosphorus stoichiometry of plant communities in geochemically P-enriched soils in a subtropical mountainous region, SW China. Environ Earth Sci 74:3867-3876. <https://doi.org/10.1007/s12665-015-4519-z>
43. Yang X, Liu Y, Wu F, Jiang X, Yu L, Wang Z, Zhang Z, Jian M, Chen G, Wei Y (2018) Quantitative trait loci analysis of root traits under phosphorus deficiency at the seedling stage in wheat. Genome 61:1-27. <https://doi.org/10.1139/gen-2017-0159>

44. Yuan Z, Chen H (2015) Negative effects of fertilization on plant nutrient resorption. *Ecology* 96: 373-380. <https://doi.org/10.1890/14-0140.1>
45. Zou X, Hu Y, Wei D, Chen S, Wu P, Ma X (2019) Correlation between endogenous hormone and the adaptability of Chinese fir with high phosphorus-use efficiency to low phosphorus stress. *Chin J Plant Ecol*, 43: 139-151. <https://doi.org/17521/cjpe.2018.0201>
46. Zou X, Wei D, Wu P, Zhang Y, Hu Y, Chen S, Ma X (2018) Strategies of organic acid production and exudation in response to low-P stress in Chinese fir genotypes differing in P-use efficiencies. *Trees* 32: 897-912. <https://doi.org/10.1007/s00468-018-1683-2>

## Figures

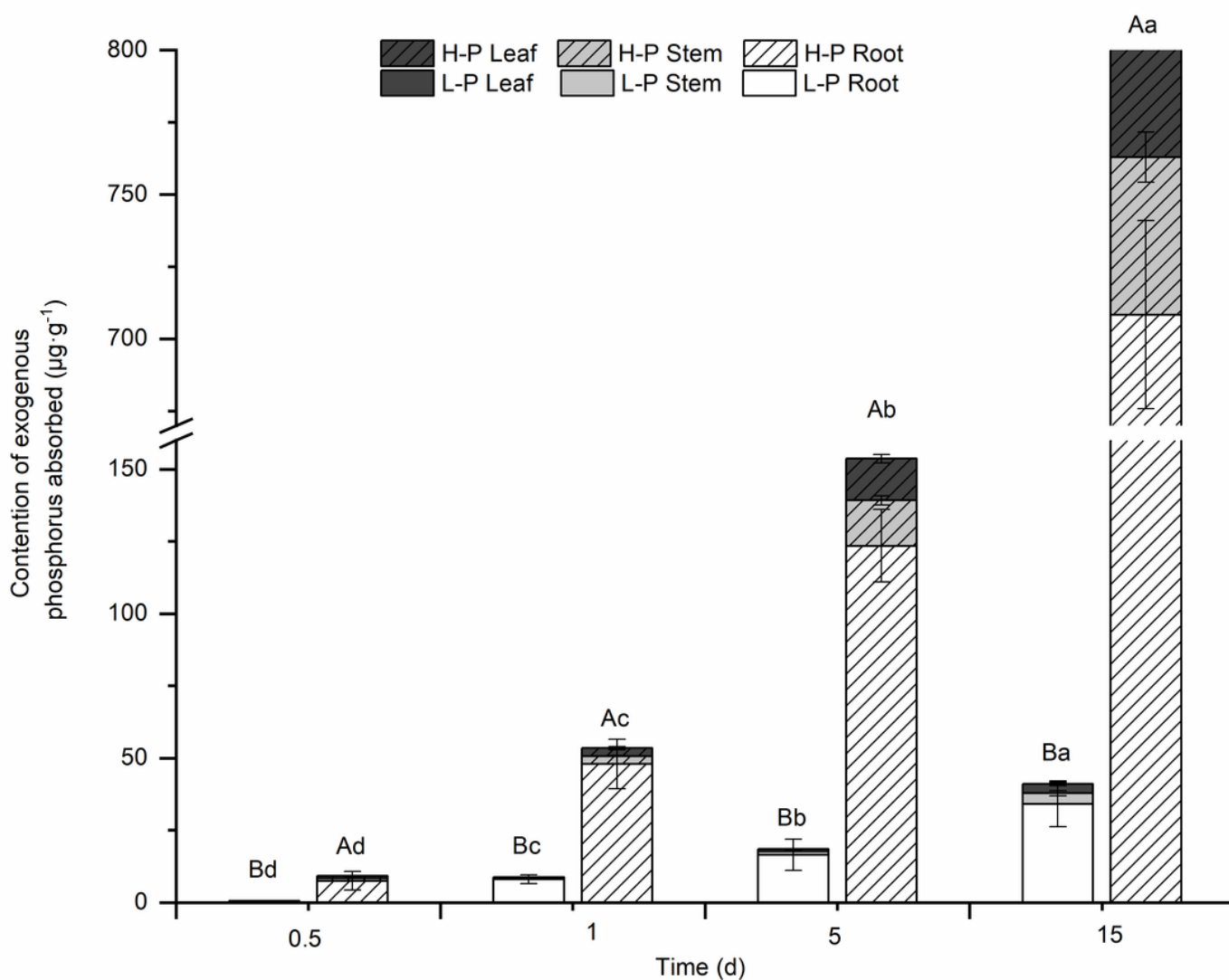
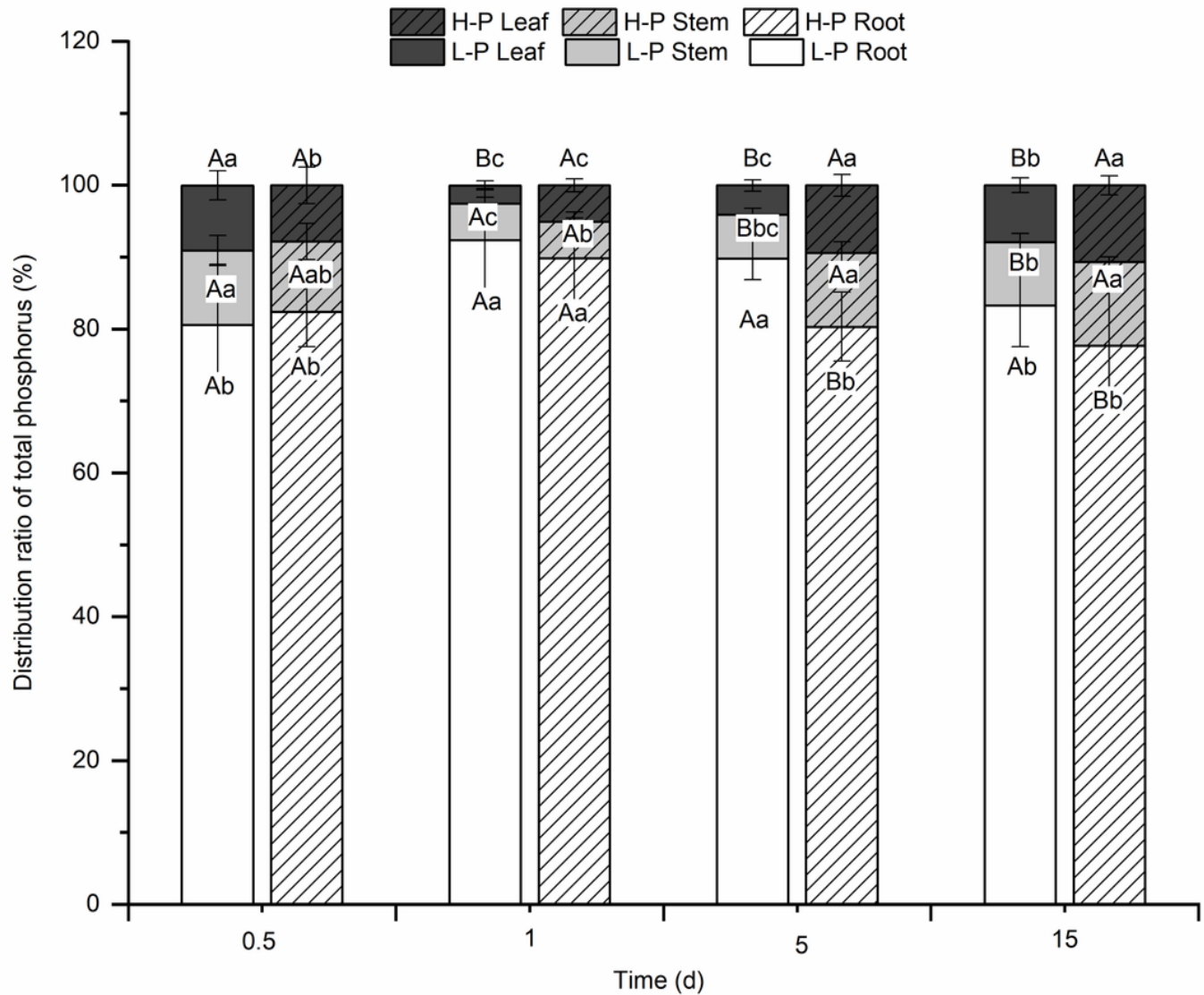


Figure 1

The content of exogenous P absorbed in different organs of M1 Chinese fir under different P supply condition. "L-P" and "H-P" represent the low-P and high-P treatment, respectively. Error bars represent standard error, and each point in the figures represents the mean of the three replicates (n=5). Lowercase letters indicate significant differences ( $P<0.05$ ) at different treatment times under the same P treatment. Uppercase letters indicate significant differences ( $P<0.05$ ) between different treatments at each time point. It showed the same labels in different organs, so we marked only one label on a bar chart



**Figure 2**

The distribution ratio of exogenous P absorbed in different organs of Chinese fir under different P supply condition. "L-P" and "H-P" represent the low-P and high-P treatment, respectively. Lowercase letters indicate significant differences ( $P<0.05$ ) at different treatment times under the same P treatment. Uppercase letters indicate significant differences ( $P<0.05$ ) between different treatments at each time point

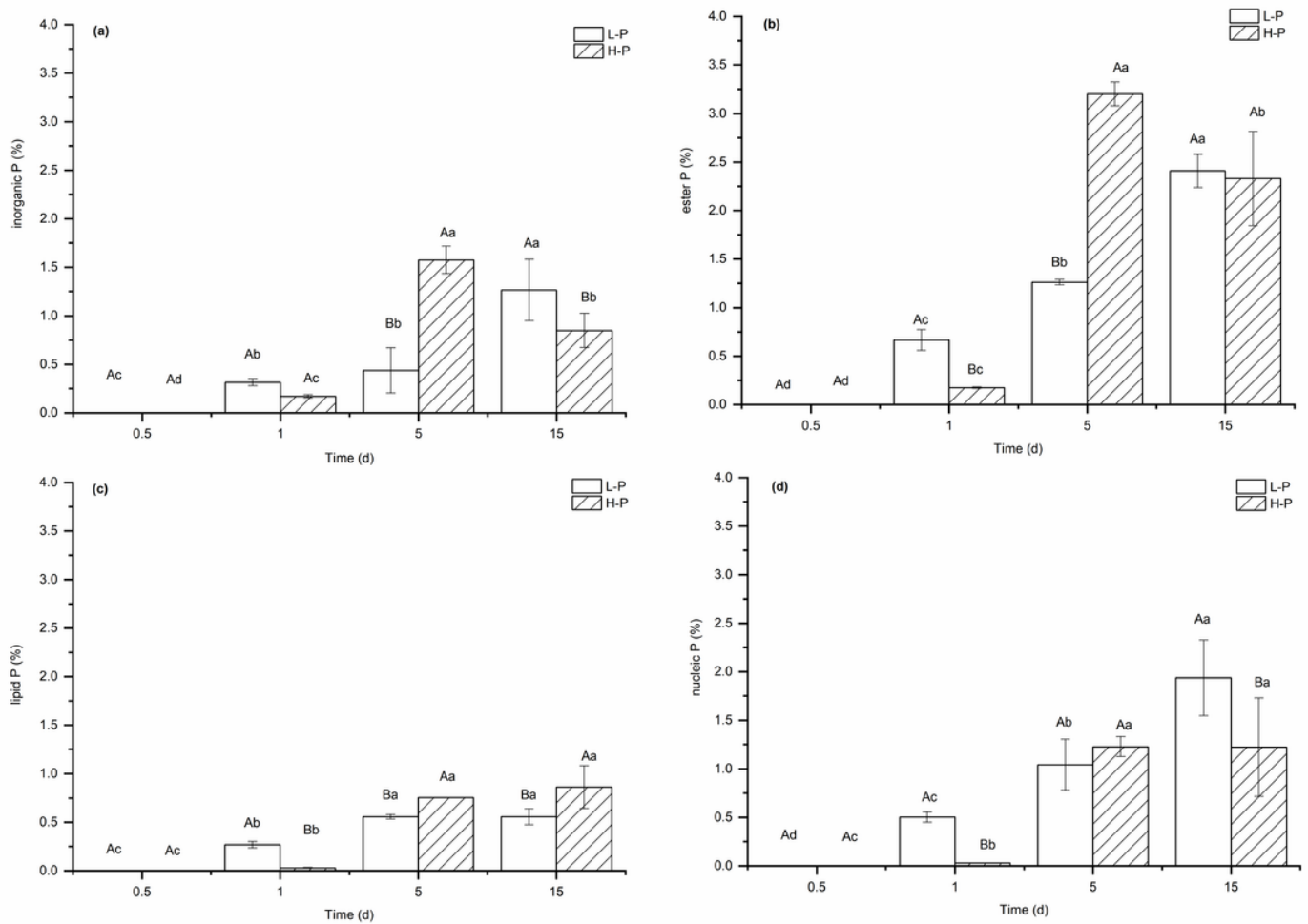


**Figure 3**

Percentage of P fractions in leaves to total plant P under high- and low-P treatments; **(a)** inorganic P, **(b)** ester P, **(c)** lipid P, and **(d)** nucleic P. "L-P" and "H-P" represent the low-P and high-P treatment, respectively. Error bars represent standard error, and each point in the figures represents the mean of the three replicates ( $n=5$ ). Lowercase letters indicate significant differences ( $P < 0.05$ ) at different treatment times under the same P treatment. Uppercase letters indicate significant differences ( $P < 0.05$ ) between different treatments at each time point

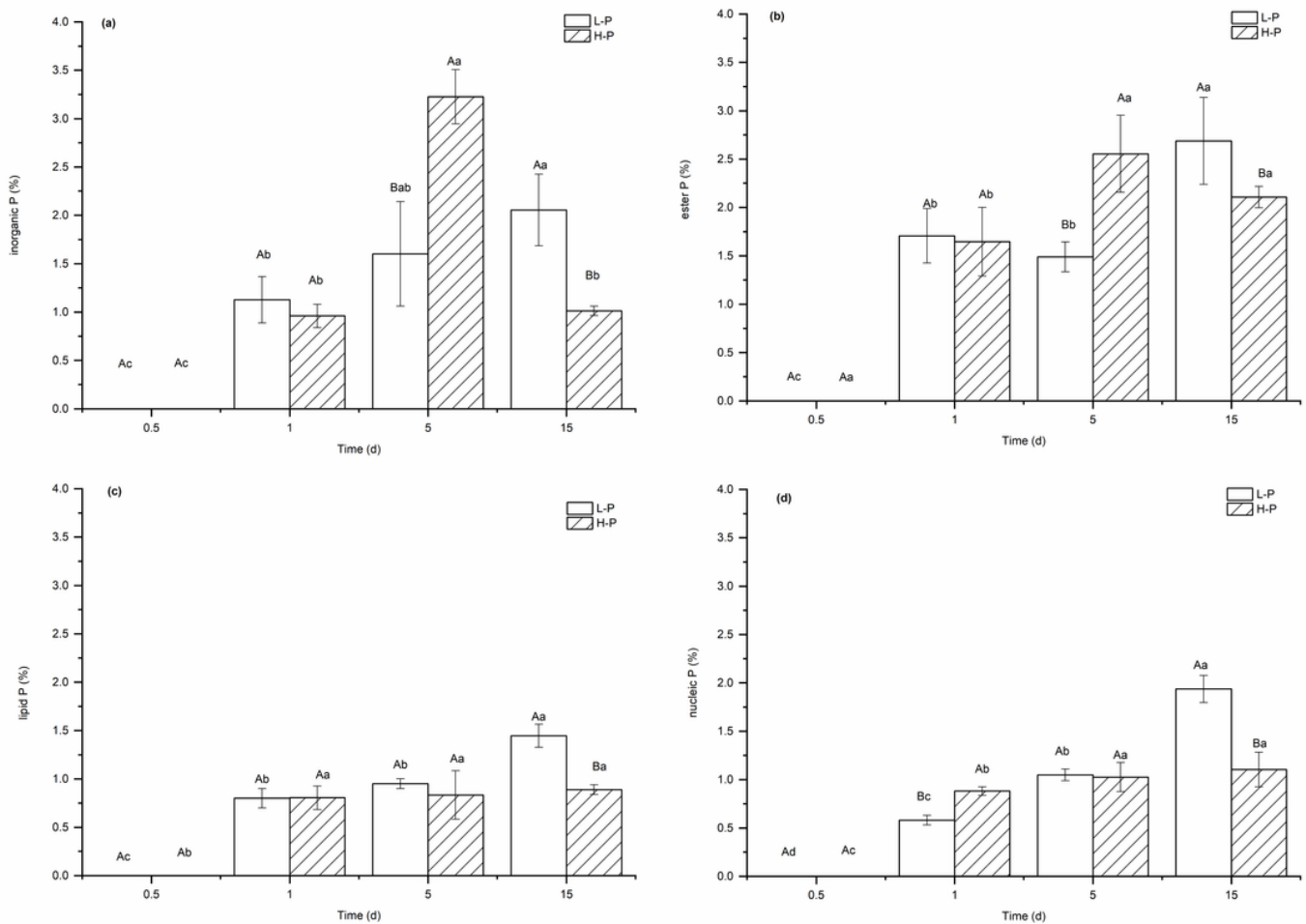


**Figure 4**

Percentage of P fractions in stems to total plant P under high- and low-P treatments; **(a)** inorganic P, **(b)** ester P, **(c)** lipid P, and **(d)** nucleic P. “L-P” and “H-P” represent the low-P and high-P treatment, respectively. Error bars represent standard error, and each point in the figures represents the mean of the three replicates ( $n=5$ ). Lowercase letters indicate significant differences ( $P < 0.05$ ) at different treatment times under the same P treatment. Uppercase letters indicate significant differences ( $P < 0.05$ ) between different treatments at each time point

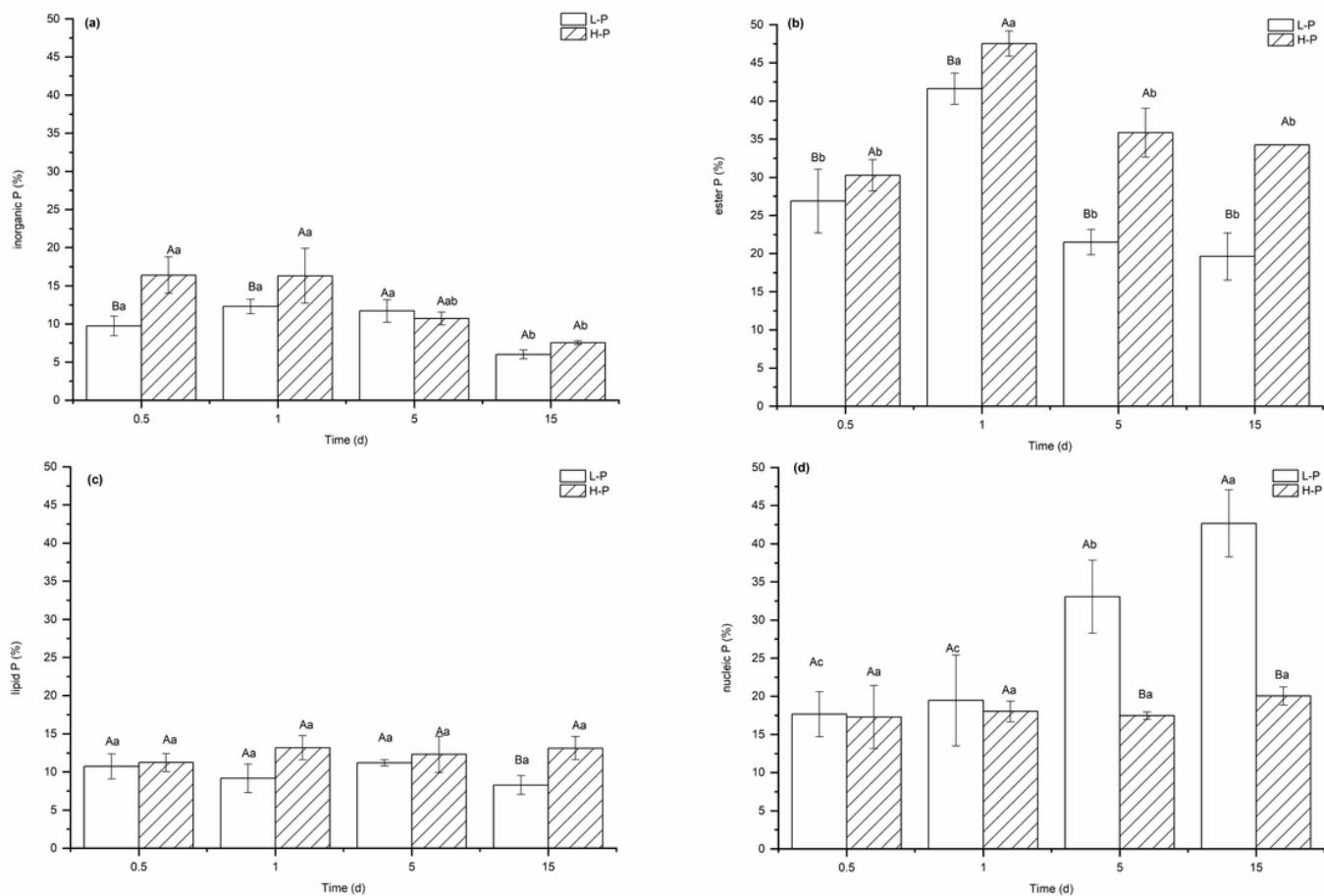


**Figure 5**

Percentage of P fractions in roots to total plant P under high- and low-P treatments; **(a)** inorganic P, **(b)** ester P, **(c)** lipid P, and **(d)** nucleic P. “L-P” and “H-P” represent the low-P and high-P treatment, respectively. Error bars represent standard error, and each point in the figures represents the mean of the three replicates ( $n=5$ ). Lowercase letters indicate significant differences ( $P < 0.05$ ) at different treatment times under the same P treatment. Uppercase letters indicate significant differences ( $P < 0.05$ ) between different treatments at each time point

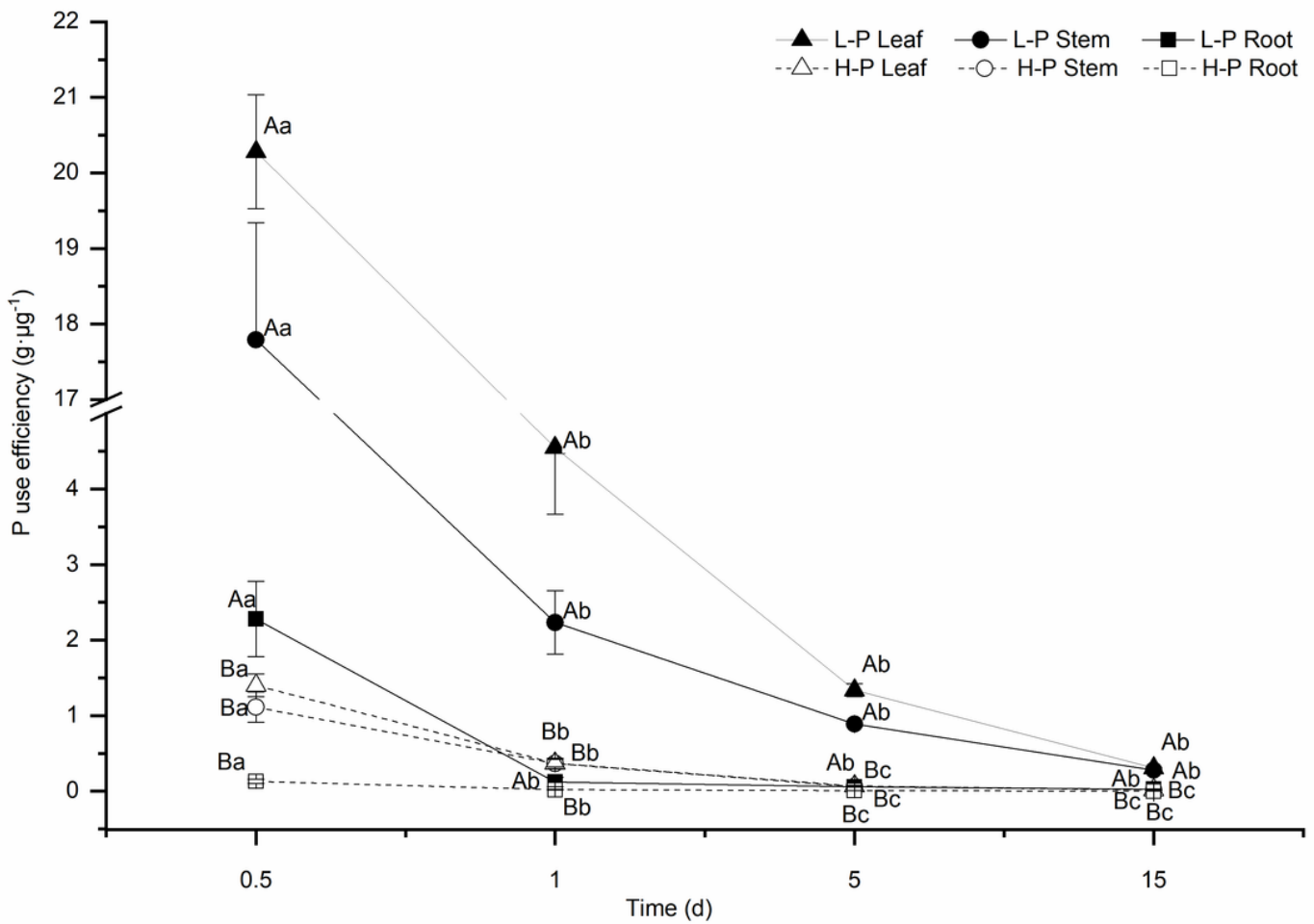


**Figure 6**

P use efficiency in different organs under high- and low-P treatments. “L-P” and “H-P” represent the low-P and high-P treatment, respectively. Error bars represent standard error, and each point in the figures represents the mean of the three replicates (n=5). Lowercase letters indicate significant differences ( $P<0.05$ ) at different treatment times under the same P treatment. Uppercase letters indicate significant differences ( $P<0.05$ ) between different treatments at each time point